Towards a Task Planning for Deformable Object Manipulation – Formulation and Computation of Linear Object Deformation

Shinichi Hirai, Hidefumi Wakamatsu, and Kazuaki Iwata

Dept. of Mechanical Engineering for Computer-Controlled Machinery,
Osaka University, Suita, Osaka 565, Japan

Abstract

A systematic approach to the static analysis of deformation of linear objects such as cords and ropes is presented. There exists many manipulative operations that deal with deformable objects in environments that robots are expected to take active parts, while rigid object manipulation has been a main interest in most of the task planning researches. Manipulative operations that deal with deformable objects is thus a challenging issue in task planning.

In this article, we will present a static analysis of the deformation of linear objects. First, the process of manipulative operations are analyzed. Secondly, a generalized coordinate system appropriate to describe the linear object deformation is introduced. Internal energy of the object and geometric constraints imposed on it are then formulated. Deformation of the object is computed by use of nonlinear programming techniques. Finally, experimental results demonstrate the effectiveness of the proposed approach.

1 Introduction

In the past decades, many researchers have been interested in task planning and many approaches and methods have been presented. Most of these works focus on manipulation of rigid objects. Namely, manipulative operations such as grasping, pick-and-place operation, assembly, and disassembly of rigid objects have been taken into consideration. Investigating manufacturing fields and viewing our living environment, however, there are many tasks that deal with deformable soft objects. For example, many manufacturing processes deal with deformable objects such as rubber tubes, sheet metals, cords, leather products, and paper sheets. There exist many deformable soft objects such as clothes and foods in our daily life. Soft tissues including muscles and skin are manipulated in medical operations. Robotic machine systems are expected to take active parts in these environments. Task planning of deformable object manipulation is thus an important research issue.

Automatic handling of deformable parts in shoe and garment manufacturing have been studies by many researchers [1]. These studies have been done for individual processes independently and few systematic approaches have been developed yet. Solid mechanics has been studied for a long time in order to analyze deformation of a solid body by investigating the relationship between stress and strain of the object [2]. It is not easy to analyze large deformation of a soft object such as paper and leather by solid mechanics approach, which basically deals with small deformation of a solid body. In computer graphics, some methods to represent shapes of curved lines and curved surfaces has been proposed [3]. Shape of cloths [4] and shape of elastic objects [5] have also been studied. These studies are not applicable to manipulative operations of deformable objects directly since they mainly focus on deformed shapes of objects and manipulation processes are not formulated there. In task planning of rigid object manipulation, global kinematics using *contact state representation* as well as kinematics and statics that characterize the unidirectional nature of mechanical contacts based on *polyhedral convex cones* have been proposed [6, 7]. They provide a coherent perspective to manipulative operations and have been applied to motion planning, control parameter design, sensing, and so on. A coherent perspective to deformable object manipulation is also required in order to develop their task planning systematically.

In this article, an analytical approach to the formulation of manipulation processes that deal with deformable linear objects such as cords and ropes is presented. First, the process of manipulative operations is described globally with regard to how a deformable object contacts with other objects around it. Secondly, a generalized coordinate system is introduced to express the deformation of a linear object. Next, internal energy of the object and geometric constraints imposed on it are formulated. Deformation of the object can be then computed by applying nonlinear programming techniques. Finally, simple experimental results are shown to demonstrate how the deformation is computed by use of the proposed approach.

2 Global Representation of Deformable Object Manipulation

Global representation of manipulation processes is on key technique to task planning of deformable object manipulation. In manipulative operations such as grasping and part-mating, mechanical contacts between objects are usually utilized in order to perform the operation successfully despite positioning errors of

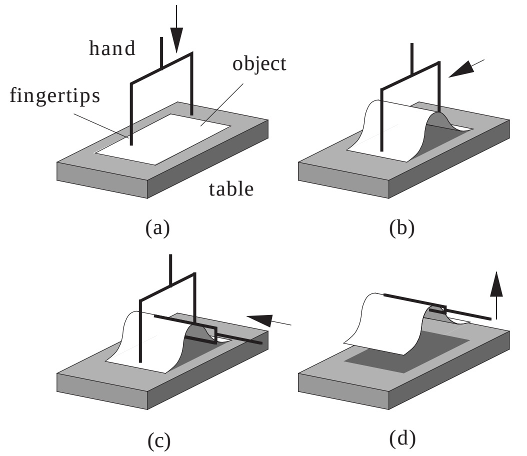

Figure 1: Example of pickup operation process

the objects. In addition to the mechanical contacts, deformation of the objects are often utilized in order to accomplish deformable object manipulation. For example, bending a thin object such as paper and a sheet metal is one effective strategy to pick up the object on a flat horizontal table. Unexpected deformation of the object sometimes brings on the failure of manipulative operations. It is thus important to describe the deformation of the objects and the contacts between them during the manipulation processes so that we can evaluate the manipulative operations.

Let us consider how the processes of deformable object manipulation are represented by taking a simple operation illustrated in Figure 1. This figure shows one operation to pickup a thin object on a flat table by a hand, which consists of four contact states. At individual contact states, the geometric constraints imposed on the object by the table and the fingertips differ topologically one another. Namely, boundary conditions of the object are different from one another at individual states. Transitions from one state to another are corresponding to operations that change the geometric constraints imposed on the object. Transition from state (a) to state (b), for example, corresponds to the operation of contacting fingertips to the object while transition from state (c) to state (d) expresses the operation of releasing the fingertips form the object. Individual states represent operations that cause deformation and motion of the object. State (b) shown in the figure, for example, corresponds to the operation of bending the object while state (d) describes the operation of moving the object upward by lifting fingertips.

From the above discussion, we find that the whole process of deformable object manipulation is described by a *Contact State Graph*, where contact states are expressed by nodes of the graph and state transitions are given by arcs connecting corresponding nodes. Nodes of the graph correspond to contacting and releasing operations while its arcs correspond to deformation and moving operations. Any manipulative operation is then given by a series of basic operations corresponding to nodes and arcs of the graph.

3 Formulation of Deformation of Linear Objects

3.1 Geometric Representation

As mentioned in the previous section, contact state graphs have a capability of representing the whole manipulation processes at a topological level. However, individual operations, especially deformation operations, must be investigated in detail so that the manipulative processes can be evaluated in advance. In this section, we will formulate the deformation of a linear object in three-dimensional space. We will extend an approach developed in [8], where one-directional planar bend deformation under geometric constraints has been formulated. Here, deformation of a linear object in three-dimensional space under not only geometric constraints but also static constraints will be discussed. The deformations are formulated by the following steps:

Step 1. Introduce generalized coordinates that can describe the natural shape and the deformed shape of the object.

Step 2. Formulate physical quantities of the object.

Step 3. Formulate interactions with other objects surrounding the linear object.

Let us introduce the generalized coordinate system expressing the deformation. Let L be the length of the object and s be the distance from one endpoint of the object along it. In order to describe the object shape, we will introduce a coordinate system fixed on space; $O - xyz$. Let $\boldsymbol{x}(s) = [x(s), y(s), z(s)]^T$ be spatial coordinates corresponding to a point $P(s)$ on the object. Now, let us focus on the bend deformation of the object by ignoring its extensional deformation. Then, the magnitude of the derivative of $\boldsymbol{x}(s)$ with respect to s must be equal to 1, that is, $\|d\boldsymbol{x}/ds\| = 1$, since the object has no extensional deformation. Parametric representations such as Bésier curves or spline curves, which are commonly used in computer graphics, do not always satisfy the above equation. This implies that these representations have a capability of describing the deformed shape alone rather than the deformation. Namely, in order to describe the object deformation, the relationship between the natural shape and the deformed shape of the object should be represented.

In order to describe the bend deformation of a linear object, we will introduce a local object coordinates, say $P - \xi\eta\zeta$, at individual points on the object, as shown in Figure 2. Select the direction of coordinates so that the ξ-axis, η-axis, and ζ-axis are parallel to x-axis, y-axis, and z-axis, respectively, in natural state. Bend deformation of the object is then given by the relationship between the local coordinates at each point and the global coordinates. Let us describe the orientation of the local coordinate system with respect to the space coordinate system by use of Eulerian angles,

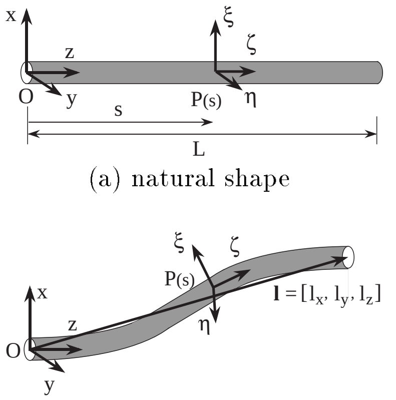

Figure 2: Coordinate systems that describe relationship between natural shape and deformed shape

$\phi(s)$, $\theta(s)$, and $\psi(s)$. The rotational transformation from $P-\xi\eta\zeta$ to $O-xyz$ is expressed by the following rotational matrix:

$$\begin{bmatrix} \mathrm{C}_\theta\mathrm{C}_\phi\mathrm{C}_\psi - \mathrm{S}_\phi\mathrm{S}_\psi & \mathrm{C}_\theta\mathrm{S}_\phi\mathrm{C}_\psi + \mathrm{C}_\phi\mathrm{S}_\psi & -\mathrm{S}_\theta\mathrm{C}_\psi \\ -\mathrm{C}_\theta\mathrm{C}_\phi\mathrm{S}_\psi - \mathrm{S}_\phi\mathrm{C}_\psi & -\mathrm{C}_\theta\mathrm{S}_\phi\mathrm{S}_\psi + \mathrm{C}_\phi\mathrm{C}_\psi & \mathrm{S}_\theta\mathrm{S}_\psi \\ \mathrm{S}_\theta\mathrm{C}_\phi & \mathrm{S}_\theta\mathrm{S}_\phi & \mathrm{C}_\theta \end{bmatrix}$$

For the sake of simplicity, $\cos\theta$ and $\sin\theta$ are abbreviated as C_θ and S_θ, respectively. A unit vector along ζ-axis at the natural state are transformed into the following vector due to the object deformation:

$$\boldsymbol{\zeta}(s) \triangleq \begin{bmatrix} -\sin\theta\cos\phi \\ \sin\theta\sin\phi \\ \cos\theta \end{bmatrix} \tag{1}$$

Since the above vector coincides to the derivative $d\boldsymbol{x}/ds$, the spatial coordinates can be computed by integrating it. Namely,

$$\boldsymbol{x}(s) = \int_0^s \boldsymbol{\zeta}(s)ds + \boldsymbol{x}_0 \tag{2}$$

where $\boldsymbol{x}_0 = [x_0, y_0, z_0]^T$ denotes the spatial coordinates at the endpoint corresponding to $s=0$. Note that this representation satisfies $\|d\boldsymbol{x}/ds\| = 1$.

Extensional deformations can be taken into consideration by introducing a strain at each point $P(s)$. Let ε be extensional strain at point $P(s)$ on a linear object along its central axis. A unit vector along ζ-axis at the natural state are transformed into $(1-\varepsilon)\boldsymbol{\zeta}(s)$ due to the object deformations. The spatial coordinates are computed by integrating $(1-\varepsilon)\boldsymbol{\zeta}(s)$ instead of $\boldsymbol{\zeta}(s)$ in eq.(2).

From the above discussion, we find that the geometrical shape of a deformed linear object can be represented by four variables, that is, Eulerian angles ϕ, θ, and ψ as well as extensional strain ε. Note that each variable depends upon parameter s.

3.2 Formulation of Internal Energy

Variational principles developed in analytical mechanics are useful to formulate physical properties of a linear object using the introduced generalized coordinates [9]. In this article, we will derive a statically stable shape of the object by applying the variational principle for statics. Dynamical effects during operations is assumed to be negligible. Let U be the potential energy of the object and W be the work done by external forces applied to the object. The variational principle for statics is given by

$$\delta(U - W) = 0 \tag{3}$$

where δ denotes variational operator. The above equation implies that the internal energy $U - W$ of the object reaches to its minimum at its statically stable shape. In other words, the stable shape can be computed by solving the minimization problem.

Let us first formulate the potential energy of a linear object. Assume that the thickness and the width of the object is negligibly small. Applying Bernoulli and Navier's assumption, the potential energy U is described as follows:

$$U = U_{flex} + U_{tor} + U_{ext} + U_{grav} \tag{4}$$

where U_{flex}, U_{tor}, and U_{ext} represent flexural energy, tortional energy, and extensional energy of the object, respectively, and U_{grav} denotes its gravitational energy.

Let us describe the curvature of the object and its tortional angle, which are originated from differential geometry [10], in order to express bend and twist deformations. Let κ and ω be the curvature and the tortional angle at point $P(s)$, respectively. The curvature and the tortional angle can be described by use of Eulerian angles as follows:

$$\begin{aligned} \kappa^2 &= \left(\frac{d\theta}{ds}\right)^2 + \sin^2\theta\left(\frac{d\phi}{ds}\right)^2 \\ \omega^2 &= \left(\frac{d\phi}{ds}\cos\theta + \frac{d\psi}{ds}\right)^2. \end{aligned}$$

Assume that bending moment and twisting moment are proportional to curvature and tortional angle at each point $P(s)$, respectively, over the object. The flexural energy and the tortional energy are then described as follows:

$$\begin{aligned} U_{flex} &= \int_0^L \frac{1}{2}R_f\kappa^2 ds \\ U_{tor} &= \int_0^L \frac{1}{2}R_t\omega^2 ds \end{aligned}$$

where R_f and R_t represent the flexural rigidity and the tortional rigidity at point $P(s)$, respectively. Assuming that extensional force is proportional to external strain at each point $P(s)$, extensional energy is given as follows:

$$U_{ext} = \int_0^L \frac{1}{2}R_e\varepsilon^2 ds$$

where R_e denotes the extensional rigidity of the object. The gravitational energy is given by

$$U_{grav} = \int_0^L Dx\ ds$$

where D represents weight per unit length of the object. Note that quantities R_f, R_t, R_e, and D may vary with respect to variable s.

Finally, let us formulate the work done by external forces. Suppose that an external force $\boldsymbol{F}_k$ is applied to the object at point $P(s_k)$. Note that coordinates corresponding to $P(s_k)$ at natural shape are given by $\boldsymbol{x}_0(s_k) = [0, 0, s_k]^T$. Thus, the work done by force $\boldsymbol{F}_k$ is described as $\boldsymbol{F}_k^T\{\boldsymbol{x}(s_k) - \boldsymbol{x}_0(s_k)\}$. Assuming that n external forces are applied to the object, the resultant work done by these forces is described as follows:

$$W = \sum_{k=1}^{n} \boldsymbol{F}_k^T\{\boldsymbol{x}(s_k) - \boldsymbol{x}_0(s_k)\} \tag{5}$$

where $\boldsymbol{F}_1$ through $\boldsymbol{F}_n$ are predefined forces acting on the object at point $P(s_1)$ through $P(s_n)$, respectively.

From the above discussion, we find that the external energy of the object as well as the work done by external forces can be described by use of the introduced generalized coordinates.

3.3 Geometrical Constraints

Due to the interaction between a linear object and other objects such as fingertips and obstacles, some geometric constraints are imposed on the object. Let us derive the geometric constraints imposed on the object. The relative position between some points on the object is often controlled during object operations. Consider a constraint that specifies the positional relationship between two points on the object. Let $\boldsymbol{l} = [l_x, l_y, l_z]^T$ be a predetermined vector describing the relative position between two operational points, $P(s_a)$ and $P(s_b)$. The following equational condition must be then satisfied:

$$\boldsymbol{x}(s_b) - \boldsymbol{x}(s_a) = \boldsymbol{l}. \tag{6}$$

The orientation at some points of the object must be also controlled during the operation. These orientational constraints are simply described as follows:

$$\phi(s_c) = \phi_c, \quad \theta(s_c) = \theta_c, \quad \psi(s_c) = \psi_c \tag{7}$$

where ϕ_c, θ_c, and ψ_c are predefined angles at one operational point $P(s_c)$.

Contact between a linear object and rigid obstacles in operation space also yields other geometric constraints. Note that any points on the object must be located outside each obstacle or on it. Let us describe the surface of an obstacle fixed on space by function $h(\boldsymbol{x}) = 0$. Assume that value of the function is positive inside the obstacle and is negative outside it. The condition that a linear object is not interfered with this obstacle is then described as follows:

$$h(\boldsymbol{x}(s)) \leq 0, \quad \forall s \in [0, L]. \tag{8}$$

Note that the condition that an object is not interfered with obstacles is described by a set of inequalities, since mechanical contacts between the objects constrain the object motion unidirectionally.

From the above discussion, we find that the geometric constraints imposed on a linear object are given by not only equational conditions such as eqs.(6) and (7) but also inequality conditions such as eq.(8). The deformed shape of the object is, therefore, determined by minimizing internal energy $U - W$ under these geometric constraints. Namely, computation of object deformation results in a variational problem under equational and inequality conditions.

4 Computation of Deformations

Computation of the deformation of a linear object results in a variational problem, as mentioned in the previous section. One method to solve a variational problem is Euler's approach, which is based on the stationary condition in function space. Recall that the geometric constraints resulting from mechanical contacts are unidirectional and are mathematically described by inequalities such as eq.(8). These conditions are nonholonomic constraints [11]. Thus, the shape of an object that minimizes potential energy does not necessarily satisfy the stationary condition. This implies that Euler's approach, which is based on the stationary condition, is not applicable.

In this paper, we will develop a direct method based on Ritz's method [12] and a nonlinear programming technique. Let us express functions $\phi(s)$, $\theta(s)$, $\psi(s)$, and $\varepsilon(s)$ by linear combinations of basic functions $\varphi_1(s)$ through $\varphi_n(s)$. Substituting the linear combinations, internal energy $U - W$ is described by a function of the coefficients of the linear combinations. The geometric constraints are also described by conditions involving the coefficients. In addition, discretizing eq.(8) by dividing interval $[0, L]$ into N small intervals yields a finite number of conditions. As a result, a set of the geometric constraints is expressed by equations and inequalities with respect to the coefficients. The deformation of a linear object can be then derived by computing the coefficients that minimize the internal energy under the geometric constraints. This minimization problem under equality and inequality conditions can be solved by use of a nonlinear programming technique such as multiplier method [13].

5 Numerical Example

In this section, one numerical example is shown in order to demonstrate how the proposed method computes the deformed shape of a linear object. The following set of basic functions are used in the computation:

$$\begin{aligned}
&\varphi_1 = 1, \quad \varphi_2 = s, \\
&\varphi_{2n+1} = \sin\frac{2n\pi s}{L}, \\
&\varphi_{2n+2} = \cos\frac{2n\pi s}{L}. \quad (n = 1, 2, 3, 4)
\end{aligned}$$

Assume that the length of the object L is equal to 100. In the nonlinear optimization for the computation of

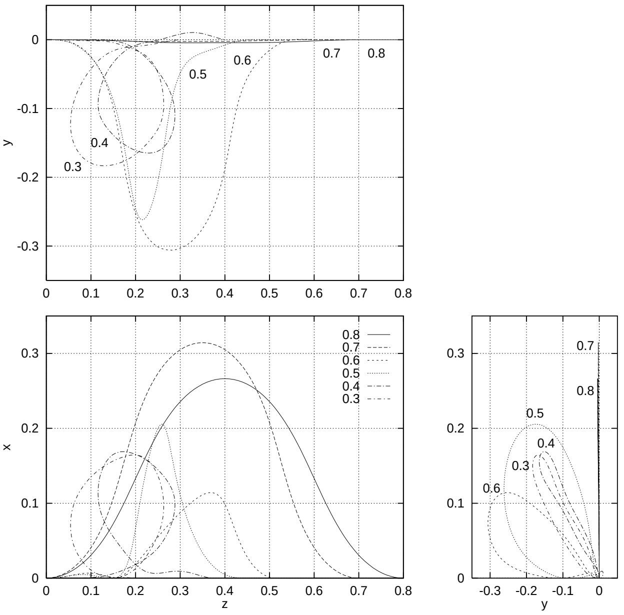

Figure 3: Example of computed deformation

deformed shapes, multiplier method and Nelder and Mead's simplex method are applied.

The example shows the deformed shapes of a linear object computed by considering its bending and torsion, say, $U = U_{flex} + U_{tor}$. Let us reduce a linear object of its length L along the central axis of the object. Suppose that the orientation at one endpoint $P(0)$ is fixed while the rotation around the central axis of the object alone is allowed at the other endpoint $P(L)$. Then, we have the following constraints:

$$\phi(0) = \theta(0) = \psi(0) = 0,$$
$$\sin\theta(L) = 0, \quad \cos\theta(L) = 1.$$

Assume that dimensionless quantity R_f/R_t, which characterizes the object shape, is equal to 100. Let us show the computed shapes corresponding to various values of the distance between two endpoints; $0.8L$, $0.7L$, $0.6L$, $0.5L$, $0.4L$, and $0.3L$. Computed shapes of the object are shown in Figure 3. Since the object shape is not planar for some values of the distance, the top view, the front view, and the side view are shown in the figure. The shape of the object is involved in x-z plane when the distance is equal to $0.8L$ or $0.7L$. The object is twisted and is not involved in any plane when the distance is equal to $0.6L$ or $0.5L$. The object contains one knot when the distance is equal to $0.4L$ or $0.3L$. Thus, it turns out that the object shape transits from a knot free shape into a one-knot shape as the distance between the endpoints decreases. Recall that the direction along the central axis of the object is fixed at both endpoints. This implies that the linear object must have a non-planar shape during this transition.

6 Experimental Results

In this section, we will compare the measured deformation and the computed deformation in order to demonstrate the validity of the proposed method. Note that the proposed method can be applied to the deformation of thin objects such as paper and sheet metals around one axis by investigating the cross section perpendicular to the axis. Let us measure the deformation of two sheets of copy paper of $92(\mu m)$ thick shown in Figure 4-(a) and (b), respectively.

Figure 4-(a) shows a rectangle of $200(mm)$ long and $30(mm)$ wide. The bend rigidity R_f and the weight D per unit length of this paper are $10^4(gw \cdot mm^2)$ and $2 \times 10^{-3}(gw/mm)$, respectively. This paper is deformed so that the distance l be 180, 140, and $70(mm)$. In the computation, we assume that angles $\theta(0)$ and $\theta(L)$ are equal to zero. The difference between the computed values and experimental values along z-axis is 11(mm) at most. The ratio of the difference to the length of the paper is approximately 6%. The difference between the computed shapes and the measurement values results from the discrepancy between the given values and the actual values of angles $\theta(0)$ and $\theta(L)$. From the measurement values, we estimate that angles $\theta(0)$ and $\theta(L)$ are actually equal to 10° and 0°, respectively. The computed values using the estimated angles are illustrated in Figure 5. The difference between the computed values and experimental values along z-axis is 2(mm) at most. Namely, the ratio of the difference to the paper length is reduced to 1%.

Figure 4-(b) shows a trapezoid of $200(mm)$ long with a left side $50(mm)$ long and a right side $100(mm)$ long. The bend rigidity R_f and the weight D of this paper can be given by $330b(gw \cdot mm^2)$ and $7b \times 10^{-5}(gw/mm)$, where b denotes the width of the paper. Note that the width b, which is given by $50 + s/4$, depends upon variable s. Thus, the bend rigidity and the weight vary according to variable s. The proposed method has a capability of computing the deformation in the case where the bend rigidity or the weight per unit length varies. Let us reduce this paper so that the distance l is equal to $160(mm)$. Without using estimated values of endpoints, the difference between the computed values and experimental values along z-axis is 8(mm) at most. The computed values using the estimated angles are illustrated in Figure 6. Note that the deformed shape of the object is unsymmetric due to the ununiformity of the bend rigidity and the weight per unit length. This figure demonstrates the proposed method can compute unsymmetric shape correctly. The difference between the computed values and experimental values along z-axis is 2(mm) at most. Namely, the ratio of the difference to the paper length is reduced to 1%.

7 Concluding Remarks

An analytical approach to the formulation of deformation of a linear object has been developed based on the physical properties of the object. First, we showed that the relationship between a natural shape of a linear object and its deformed shape should be represented in order to describe the object deformation. One generalized coordinate system was introduced so that the object deformation can be described appropriately. Secondly, internal energy and geometric constraints of the object were formulated using the introduced coordinates. It turned out that not only equational constraints resulting from predefined condition on the object motion but inequality constrains resulting from unidirectional nature of mechanical contacts are imposed on the object. Next, a procedure to compute the object deformation has been developed by applying nonlinear programming techniques. One numerical example and experimental results have demonstrated the effectiveness of the proposed approach.

References

[1] Taylor, P. M. et al., *Sensory Robotics for the Handling of Limp Materials*, Springer-Verlag, 1990

[2] Fung, Y. C., *Foundations of Solid Mechanics*, Prentice-Hall, 1965

[3] Rogers, D. F. and Adams, J. A., *Mathematical Elements for Computer Graphics*, McGraw-Hill, 1976

[4] Weil, J., *The Synthesis of Cloth Objects*, Computer Graphics, Vol 20, No.4, pp.49-54, 1986

[5] Terzopoulos, D. et al., *Elastically Deformable Models*, Computer Graphics, Vol 21, No.4, pp.205-214, 1987

[6] Desai, R. S. and Volz, R. A., *Identification and Verification of Termination Conditions in Fine Motion in Presence of Sensor Errors and Geometric Uncertainties*, IEEE Int. Conf. Robotics and Automation, pp.800–807, 1989

[7] Hirai, S. and Asada, H., *Kinematics and Statics of Manipulation Using the Theory of Polyhedral Convex Cones*, International Journal of Robotics Research, Vol.12, No.5, October, pp.434–447, 1993

[8] Hirai, S., Wakamatsu, H., and Iwata, K., *Modeling of Deformable Thin Parts for Their Manipulation*, Proc. IEEE Int. Conf. Robotics and Automation, pp.2955–2960, San Diego, 1994

[9] Crandall, S. H., Karnopp, D. C., Kurts, E. F., and Pridmore-Brown, D. C., *Dynamics of Mechanical and Electromechanical Systems*, McGraw-Hill, 1968

[10] Auslander, L., *Differential Geometry*, Harper International Edition, 1977

[11] Goldstein, H., *Classical Mechanics*, Addison-Wesley, 1980

[12] Elsgolc, L. E., *Calculus of Variations*, Pergamon Press, 1961

[13] Avriel, M., *Nonlinear Programming: Analysis and Methods*, Prentice-Hall, 1976

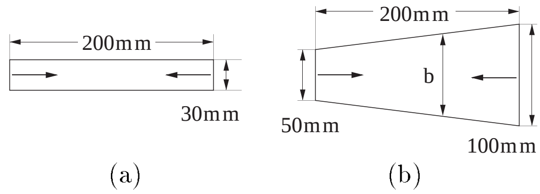

Figure 4: Experimental paper sheets

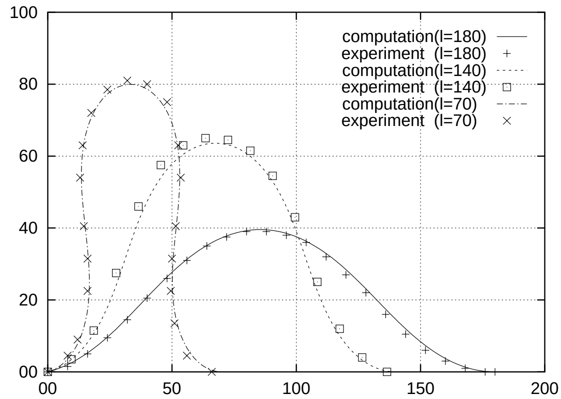

Figure 5: Computed deformed shape and measured deformed shape of rectangle paper

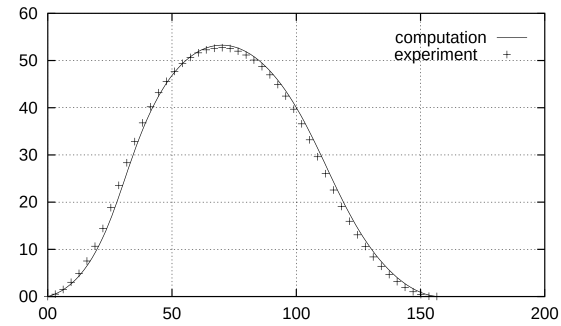

Figure 6: Computed deformed shape and measured deformed shape of trapezoid paper